Experimental study of phase change materials for photovoltaic modules: energy performance and economic yield for the EPEX spot market

Ewald Japs[a], Gerrit Sonnenrein[b], Stefan Krauter[a,*], Jadran Vrabec[b]

[a] University of Paderborn, Electrical Energy Technology – Sustainable Energy Concepts, 33098 Paderborn, Germany, Ewald.Japs@upb.de, [1]Stefan.Krauter@upb.de

[b] University of Paderborn, Thermodynamics and Energy Technology, 33098 Paderborn, Germany, Gerrit.Sonnenrein@upb.de, Jadran.Vrabec@upb.de

Keywords

phase change material, electricity spot market, photovoltaic module, cooling measure

Abstract

Cooling of photovoltaic (PV) devices increases voltage and power output, but in standard applications, cooling measures are only beneficial if the associated costs are lower than the cumulative profit. A technical and economic analysis of a passive cooling measure based on phase change materials (PCMs) is conducted here. Three PV modules, one standard reference module and two equipped with PCMs, are studied experimentally. Although both have the same melting temperature, one of the PCMs has a significantly higher thermal conductivity and a lower heat storage capacity than the other. The analysis of the present experimental data considers the energy price variation at the European Power Exchange (EPEX) spot market during the day without considering any costs. Because additional power is supplied before noon for PCM charging, favorable results are observed during this period. However, higher operating temperatures of the PV modules occur later in the day due to the thermal insulation effect of the PCM layer attached to the back side of the modules. In total, this results in a negative economic yield on most days. The PCM with a higher thermal conductivity had significantly lower temperatures after charging and a corresponding higher yield.

* Corresponding author

Nomenclature

Symbols		
c_p	Average specific isobaric heat capacity	kJ/(kg·K)
E	Energy yield	Wh
e	Relative energy yield difference	%
h	Specific enthalpy of fusion (20 °C - 30 °C)	kJ/kg
P	Electrical power output	W_p
r	Energy price	€/kWh
t	Time	s
Y	Economic yield	€
y	Relative economic yield difference	%
γ	Temperature coefficient of P_{max}	%/K
η	Conversion efficiency	%
θ	Temperature	°C
λ	Thermal conductivity	W/(m·K)
ρ	Specific density	kg/m^3
ω	Mass fraction	g/g
Δ	Difference	

Index	
d	Based on a daily trading period
eq	Equipped with PCM or PCM+
i	Counting variable
j	15 min or 1 h time block energy price
m	Melting point
max	Maximum point
n	Summation limit
ref	Reference
uq	Unequipped (no PCM or PCM+)

Abbreviation	
EPEX	European Power Exchange
ISFH	Institute for Solar Energy Research Hamelin
MPP	Maximum power point
PV	Photovoltaic
PCM	Phase change material
PCM+	Phase change material with improved thermal conductivity

STC	Standard test conditions

1. Introduction

The negative effect of elevated operating temperatures on the conversion efficiency of crystalline silicon solar cells is well known (Radziemska, 2006). Interventions to reduce operating temperatures are usually considered to increase the electrical energy yield. Low operating temperatures of photovoltaic (PV) modules also have a positive effect on degradation (Meyer and van Dyk, 2004; Junsangsri and Lombardi, 2010). Furthermore, a damping of short-term temperature fluctuations may increase PV module lifetimes (Köntges et al., 2014).

Both active cooling measures, such as water cooling on the module back (Bahaidarah et al., 2013; Moharram et al., 2013) or front side (Krauter, 2004), and passive cooling measures adapted from latent heat storage consisting of selected phase change materials (PCMs) have been investigated (Norton et al., 2011; Hasan et al., 2014). The scientific interest in using PCM for the thermal management of PV modules has increased rapidly over the last decade. Numerous experimental and computational studies have been conducted for the use of PCM to manage the temperature issues of electronic devices such as PV modules (Browne et al., 2015). Meanwhile, it is well known that the operating temperature of PV modules can be decreased significantly due to the melting of the attached PCM. However, at high temperatures, PCM layers may cause unwanted and significant thermal insulation due to their typically low thermal conductivity. One possibility of combating this problem is to mix the PCM with expanded graphite (Mehling and Cabeza, 2008).

The first investigation into integrating PCM with a PV module was conducted in 1978; this study showed that the beneficial cooling effect of PCM can be enhanced by increasing its thermal conductivity and increasing the heat transfer from the PV module to the PCM at the thermal interface (Stultz and Wen, 1977). Recently, one of the main research objectives of Huang et al. (Huang et al., 2011) was to promote the heat transfer into and out of PCM using fins within the aluminum container encapsulation. They also developed a validated numerical model for a PV-PCM module. Hasan et al. (Hasan et al., 2015) compared the effects of two different PCMs encapsulated in an aluminum container with internal fins for two different climate conditions (Dublin, Ireland and Vehari, Pakistan) using outdoor measurements and simulations using the numerical model from (Huang et al., 2011). Two main conclusions were drawn: First, the deviation between the simula-

tion and experiment results was very low in terms of the average temperatures of the front surface of both PV-PCM modules. Second, the highest temperature drop was approximately 21 K compared to the reference PV module was observed in Vehari for a PV-PCM module based on a salt hydrate.

Laboratory experiments combined with a computational study were conducted by (Jay et al., 2010). Two PV-PCM systems, a PV module with a thermally insulated back side and a reference PV module, were simultaneously exposed to three different insolation intensities (600, 800 and 1000 W/m^2) using a solar simulator. Both paraffin-based PCMs (with melting temperatures of 27 °C and 45 °C) were filled into a honeycomb aluminum structure, which was closed on both sides by an aluminum plate to promote heat transfer from the PV module. A 15-25 % increase in energy yield compared to the reference PV module due to temperature regulation was measured.
The combination of PCM-infused graphite and finned heat sinks for the thermal management of PV modules (Atkin and Farid, 2015) achieved a 13% increase in energy yield through reduced peak temperatures and a temporary time shift in the temperature rise.

In the present work, a commercial paraffin RUBITHERM® RT 28 HC with an improved thermal conductivity of λ = 2.4 W/(m·K) and the same PCM compound with the standard thermal conductivity of λ = 0.19 W/(m·K) were studied. The high thermal conductivity was achieved by adding expanded graphite to the PCM compound. Although the improved PCM (hereafter referred to as PCM+) has a reduced heat storage capacity because of a decreased mass fraction of the effective phase change material, it promises better performance and applicability. Therefore, one PV module was equipped with PCM+ and another PV module was equipped with the conventional PCM; both were compared with a standard reference PV module, simultaneously measured at outdoor summer conditions during the year 2013 in Paderborn, Germany. A technical comparison of the two PV-PCM modules was conducted to assess the temperature development and energy yield.

In general, due to the rapid decrease of PV module costs, cooling interventions are often less cost-effective in terms of direct power gain. On the other hand, the typical power generation shift to the morning hours with PV-PCM modules may nonetheless be favorable, considering the higher electricity prices before noon on the European Power Exchange (EPEX) spot market, cf. Fig. 1. In this investigation, no costs were considered, and the economic analysis focused exclusively on the yield differences due to the use of PCM and PCM+.

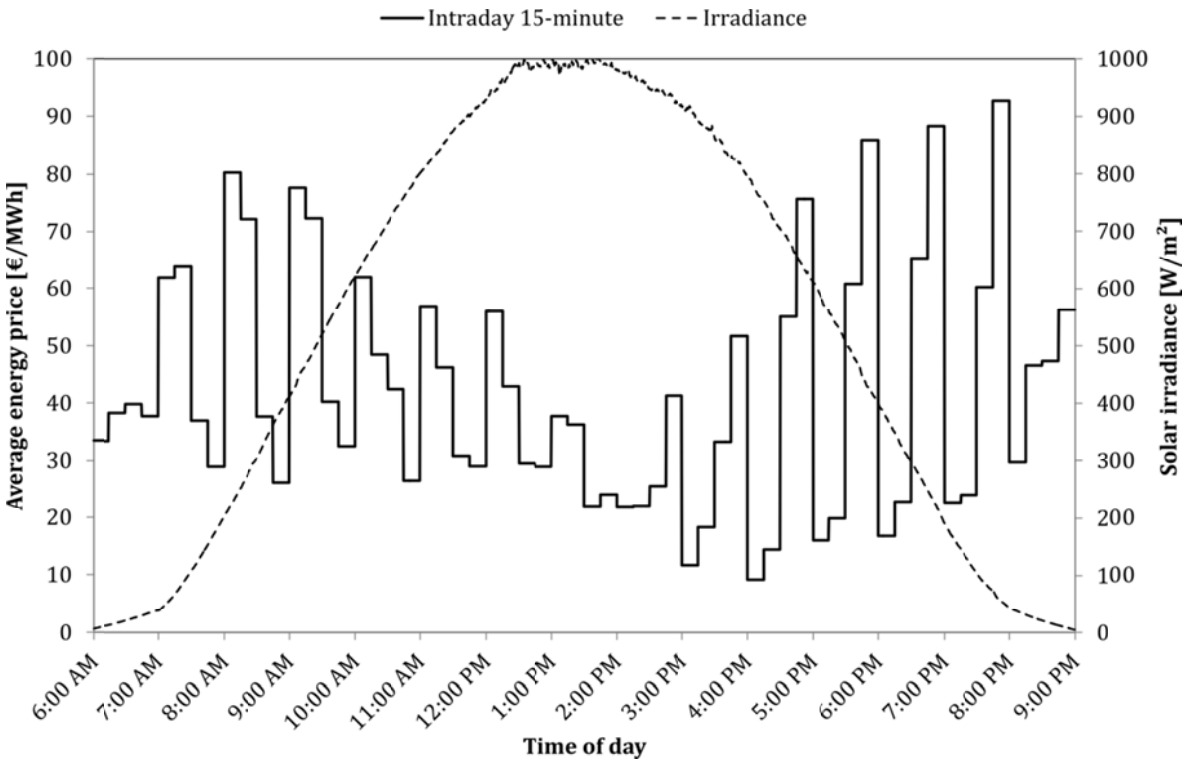

Fig. 1 Price development on the EPEX spot market (EPEX Spot SE, 2013), showing real data for Friday, August 2nd, 2013. The solar irradiance on that nearly perfect summer day as measured in Paderborn, Germany is superimposed on the graph.

2. Measurement setup

2.1. Characterization of PCM and PCM+

The applied PCM was hermetically encapsulated in bags consisting of an aluminum-polymer composite film with 500 g of PCM each. The thermal conductivity of the RUBITHERM® RT 28 HC alone was λ = 0.19 W/(m·K); this was significantly increased by adding expanded graphite (THERMOPHIT® GFG, SGL GROUP), following the work by (Sonnenrein et al., 2015). After adding graphite with a mass fraction of $\omega \approx 0.2$ g/g, the thermal conductivity of PCM+ increased by more than a factor of 12. Therefore a thermal conductivity of λ = 2.4 W/(m·K) has been measured by applying the stationary method as described in (Mehling et al., 2000). Fig. 2 shows the temperature dependence of the specific enthalpy of PCM+ compared with that of pure PCM. The underlying measurements were conducted with heat flow 3-layer-calorimeter (WOTKA, W&A) (Kenfack and Bauer, 2014) specifically developed for analyzing PCM and for validation additionally with Differential Scanning Calorimetry (DSC, TG-DSC 111, SETARAM) (Sarwar and Mansoor, 2016). Compared to common DSC devices, WOTKA allows increased sample quan-

tities of up to 100 g what is of particular importance to determine the phase change temperature of composites. Therefore, the study shows in the following the experimental results of the 3-layer-calorimeter measurements.

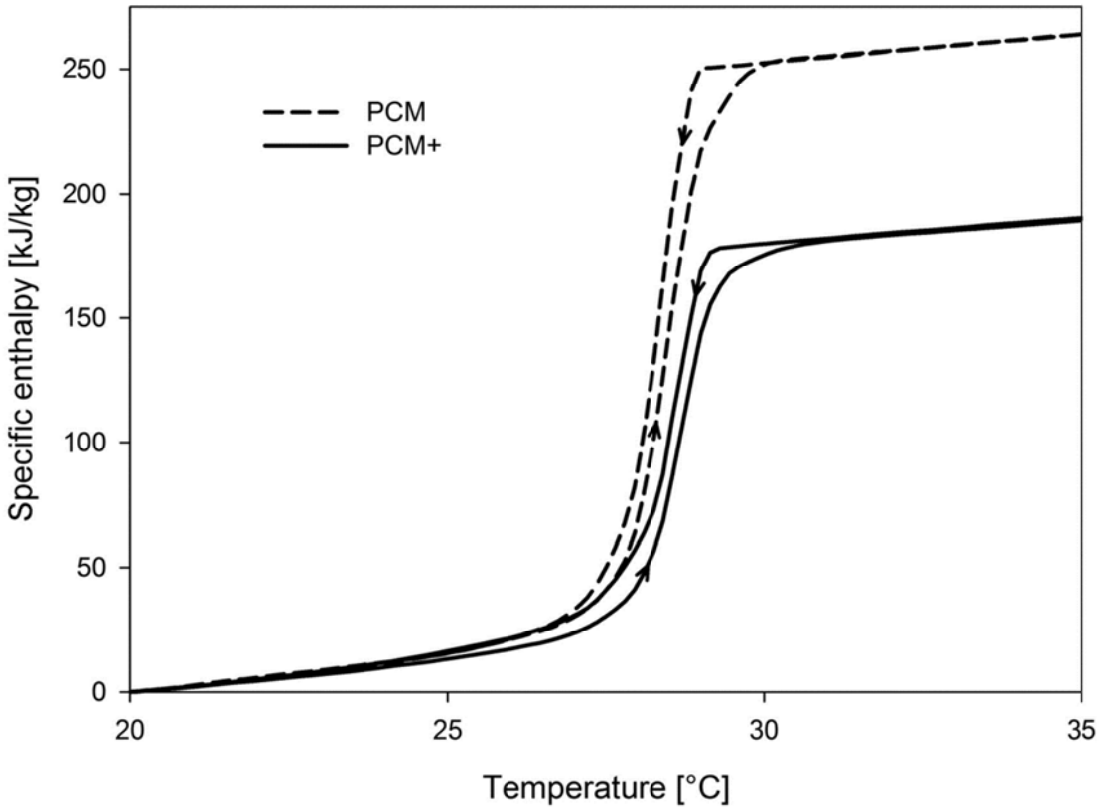

Fig. 2 Specific enthalpy as a (hysteresis) function of temperature for PCM and PCM+.

The heat storage capacity of the compounded material is lower than that of pure PCM due to its significant graphite content. Over the temperature range of 20 °C to 35 °C, the specific heat storage capacity was thus reduced by approximately 28%, from 260 kJ/kg to 185 kJ/kg. The melting temperature remained unaffected at approximately 28 °C. It should be noted that the paraffin used here shows no significant sub-cooling, unlike common salt hydrates. Based on the measured PCM properties, the amount of storable heat per PV module over the temperature range of 20 °C to 35 °C was approximately 391 kJ for PCM and approximately 275 kJ for PCM+ (cf. Fig. 2 and Table 1).

2.2. Modules and measurement setup

Two of the three technically identical multi-crystalline silicon PV modules were equipped with three PCM bags each. First, one Pt100 foil resistance thermometer with

an accuracy of about ±0.5K (class B according to IEC 60751:2008) was attached via a thermally conductive paste, positioned at the center of a solar cell, to the back side of each PV module, as indicated in Fig. 3. Next, three macro encapsulated PCM bags were attached next to each other, where they covered approximately 80% of the solar cell area on the back side of the PV module. Another Pt100 foil resistance thermometer was placed on the air-facing surface of the PCM below the first resistance thermometer. Finally, an aluminum grid was fixed with screws at the back side of the PV module frame to tightly press the PCM bags to the PV modules. In addition, an aluminum plate was fixed below the PV outdoor laboratory framework, covering the projected area under the three PV modules at a free distance of 8 cm. However, horizontal fixation bars inhibited natural convection along the whole module, cf. Fig. 4. This measure was added to equalize convective heat transfer i.e., to reduce the impact of wind blowing along the back side of the module. Moreover, this condition simulated a PV rooftop installation. Measurements were conducted from early July to mid-August of 2013.

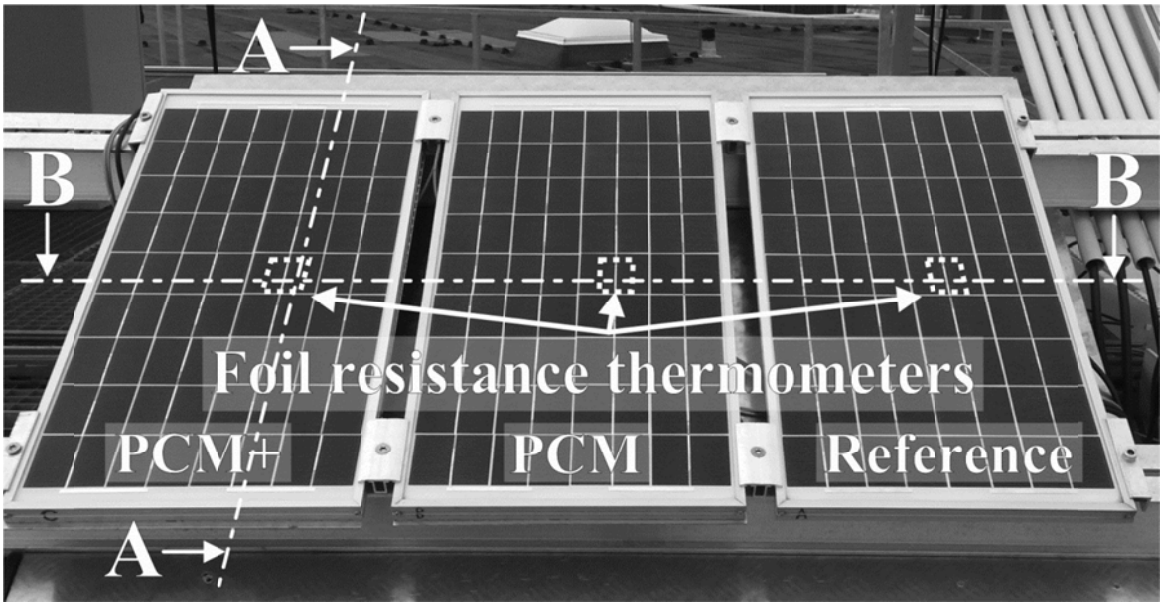

Fig. 3 Experimental setup in Paderborn, Germany, cf. Fig. 4 for cross sections A-A and B-B.

The three modules were installed in the PV outdoor laboratory of the University of Paderborn, Germany (51°45’ 23.87” N, 8°38’ 38.43” E) with an inclination of 30° to the horizontal and an azimuth of 0°, as shown in Fig. 3. In addition to the surface temperatures, the short-circuit current, open-circuit voltage and MPP power output were measured and logged simultaneously every 10 s for each PV module by an in-house developed electrical load with a MPP-error of about ±1%. Furthermore, global irradiance in the plane of the PV modules was measured using a calibrated pyranometer (CMP 21, Kipp &

Zonen).

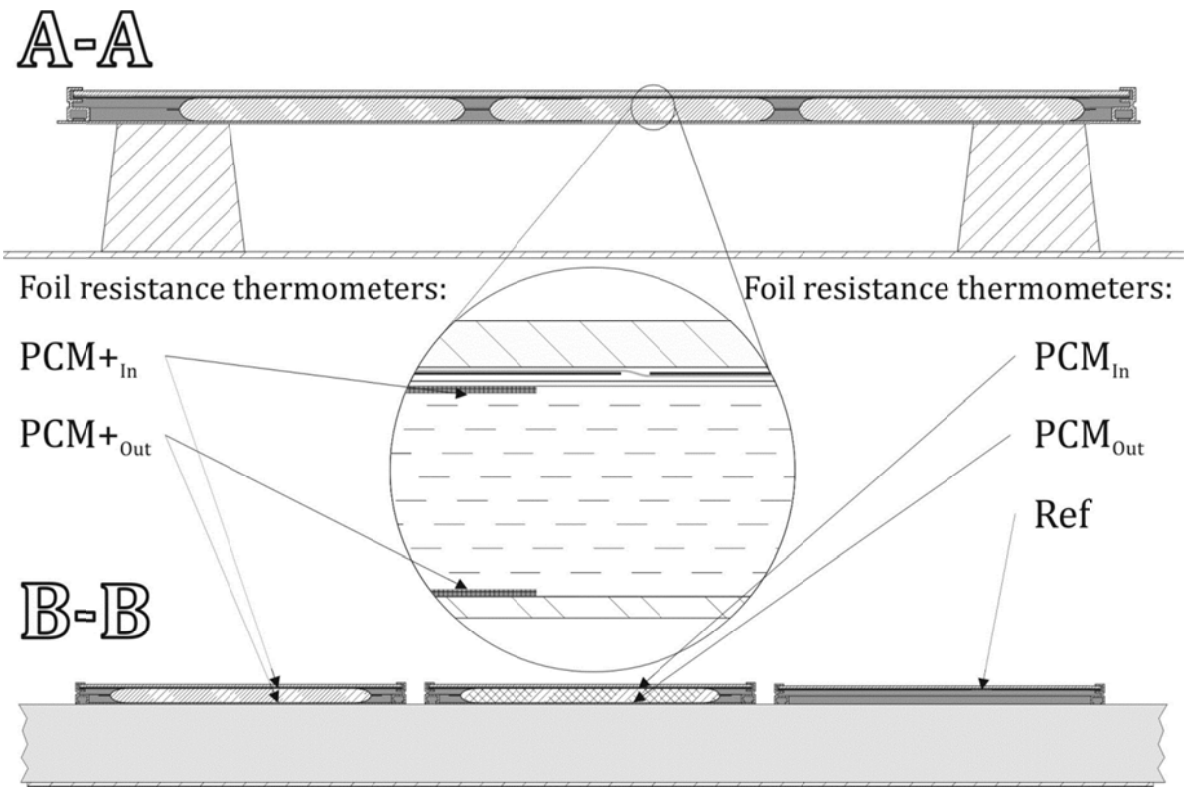

Fig. 4 Cross section schematic of the measurement setup, as illustrated in Fig. 3, indicating the positions of the foil resistance thermometers.

Prior to their installation, the PV modules were measured under standard test conditions (STC) at the Institute for Solar Energy Research Hamelin (ISFH). All relevant parameters of the investigated PCM and modules are listed in Tables 1 and 2.

Table 1: Properties of the investigated PCMs.

Property	**Symbol**	**PCM**	**PCM+**	**Units**
Specific enthalpy of fusion (20 °C - 30 °C)	h	235	158	kJ/kg
Average specific isobaric heat capacity	c_p	2.3	2.2	kJ/(kg·K)
Specific density	ρ	760	890	kg/m^3
Thermal conductivity	λ	0.19	2.4	W/(m·K)
Melting temperature	θ_m	28	28	°C

Table 2: Parameters of the investigated PV modules under STC.

Electrical parameter	**Symbol**	**Reference**	**PCM**	**PCM+**	**Units**
Maximum power output	P_{max}	28.3	26.6	28.8	W_p
Conversion efficiency	η	12.1	11.4	12.4	%

Temperature coefficient of P_{max}	γ	-0.41	-0.40	-0.42	%/K

Significant differences in the temperature coefficient of the power output and conversion efficiency were detected among the three PV modules, so the measured energy yield of the PV-PCM modules cannot be directly compared. Therefore, the following basic assumptions were made to ensure a satisfactory comparability of the results:

- All three PV modules have the same operating temperature at identical operating conditions.
- Differences between the measured temperature values are caused exclusively by the attached PCM or PCM+ bags.
- The temperature values measured by the thermometers Ref, PCM_{In} and $PCM+_{In}$ represent the operating temperature of the corresponding module.

The measured temperature of the Ref thermometer was used as a reference value for comparison. Thus, the measured electrical power output of the PCM module as well as that of the PCM+ module was adjusted according to the measured temperature of the Ref thermometer and the temperature coefficient of the PCM and PCM+ modules given in Table 2. A detailed description of these adjustments is given in Section 3.2.

3. Energy performance and economic yield

3.1. Influence of PCM on temperature

Due to the strong influence of the PCM on the temperature of the PV modules, a detailed analysis of the measured diurnal temperature variations is necessary. For this purpose, two days with high insolation and very clear sky conditions were selected. Both conditions were fulfilled on the 1st and 2nd of August 2013. The surface temperatures measured on these days are shown in Fig. 5 as a function of time.

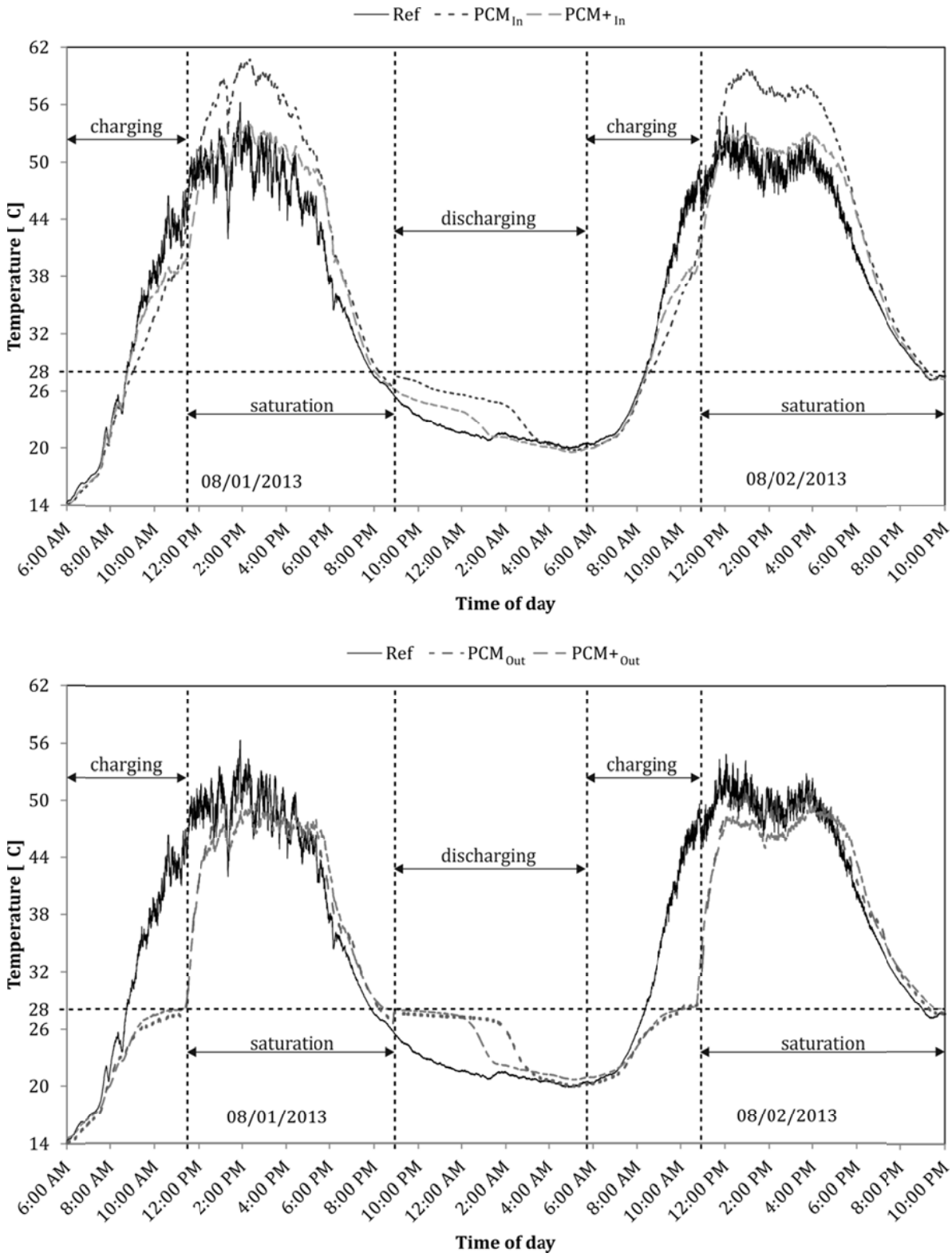

Fig. 5 Surface temperatures of the reference module and the inner (top) and outer (bottom) surface temperatures of the PCM and PCM+ modules on August 1st and 2nd, 2013.

Fig. 5 shows that the modules equipped with PCM and PCM+ exhibit temperature variations with significantly lower fluctuations than the reference PV module. As expected, the operating temperatures decreased during the melting of the PCM, as indicated by

"charging" in Fig. 5. Coincidentally, the melting processes of PCM and PCM+ terminated at approximately the same time. After complete melting, the PCM temperature increased more rapidly than that of PCM+ due to the higher thermal resistance to heat transfer through the PCM package; both temperatures increased above the temperature of the reference PV module. During the saturation stage, a smaller difference occurred between $PCM+_{In}$ and the $PCM+_{Out}$ surface temperatures compared to the temperature difference between PCM_{In} and PCM_{Out}, cf. Fig. 5. In addition, it can be concluded that the increased thermal conductivity of PCM+ leads to significantly lower operating temperatures after complete melting. Finally, it was observed that PCM needed approximately 4 h for complete solidification, whereas PCM+ needed only approximately 3 h, which means that approximately 25% more mass of PCM+ can be solidified overnight compared to PCM.

3.2. Temperature dependent energy yield

As mentioned in Section 2.2, the surface temperature θ_{ref} of Ref was used as a reference value for calculating the power differences caused by PCM and PCM+. Explicitly considering the differences between the electrical parameters of the studied modules (cf. Table 2), the hypothetical electrical power output P_{uq} of the PCM and PCM+ modules *without* the attached phase change material was determined according to equation (1). The temperature variation due to the presence of the phase change material ($\theta_{eq} - \theta_{ref}$) was measured by the thermometers PCM_{In} and Ref or $PCM+_{In}$ and Ref. The measured electrical power output of the modules is denoted by P_{eq}

$$P_{uq} = P_{eq} - \gamma \cdot P_{max} \cdot \left(\theta_{eq} - \theta_{ref}\right) \tag{1}$$

where γ is the temperature coefficient of maximum power output. Based on these power output values, all days within the measurement period were analyzed by applying the following three steps:

- First, the temperature dependent energy differences were determined.
- Second, they were weighted with the EPEX spot market price.
- Third, four energy economic difference values for the comparison of the PV-PCM modules were defined for each day.

Because the measured data were recorded every Δt=10 s, it was necessary to assume constant values until the next sampling. Thus, the power output values P_{eq} and P_{uq} were multiplied by Δt to obtain the generated energy E_{eq} and E_{uq} over Δt. Subsequently, the

E_{eq} and E_{uq} values were then added into the 15 min blocks $\bar{E}_{eq}$ and $\bar{E}_{uq}$, consisting of 90 energy values each

$$\bar{E}_k = \sum_{i=1}^{n} E_{k,i} \qquad \text{with } k = eq \text{ or } uq. \tag{2}$$

To compare the PCM, the relative energy yield difference e was determined by

$$e = \frac{\bar{E}_{eq} - \bar{E}_{uq}}{\bar{E}_{uq}}. \tag{3}$$

Illustrating the applied procedures, the measured data of August 2nd, 2013 were used for an example comparison. The resulting diurnal variation of the relative contribution of PCM and PCM+ on the energy yield as well as of the insolation at the PV module level is shown in Fig. 6.

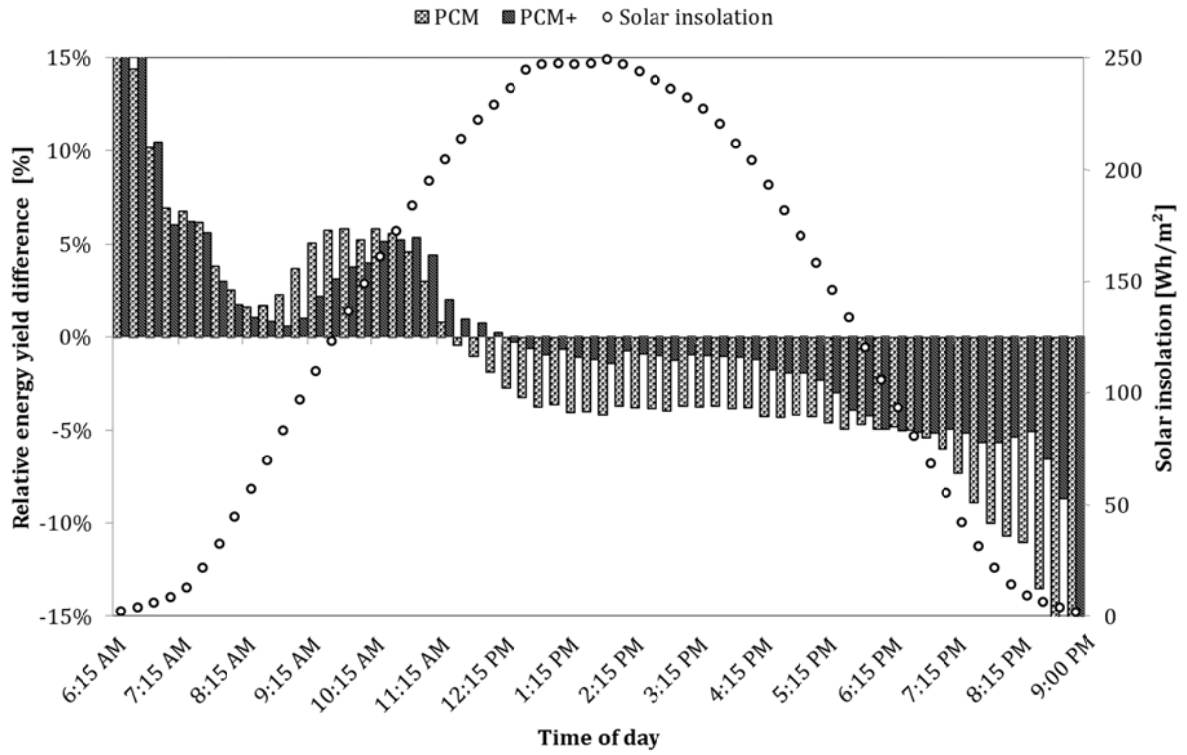

Fig. 6 Example daytime dependent relative energy yield differences of PV modules equipped with PCM or PCM+ vs. the reference PV module (baseline) on August 2nd, 2013. The cumulative solar insolation values over 15 min are plotted in superposition.

3.3. Economic evaluation

For the second step, the following boundary conditions were considered in the present evaluation:

- Electrical energy is traded on the EPEX intraday spot market of Germany and Austria.
- Electrical energy is preferably traded in 15-min periods; 1-h period trades are also allowed.
- The generated photovoltaic electrical power equals the actual traded power at all times.
- The daily trading period ranges from 6 a.m. to 9 p.m.

Moreover, the studied modules were linearly scaled up to 10 MWp plants to comply with the prequalification requirements for EPEX trading such that the minimum trading increment volumes of 0.1 MW could be offered. Therefore, the 15-min energy blocks $\bar{E}_{eq}$ and $\bar{E}_{uq}$ were multiplied by the ratio of the assumed peak power of the PV plant and the maximum power P_{max} of the PV module. In addition, the upscaled energy blocks were monetarily weighted by real average energy prices retrieved from the EPEX online database (EPEX Spot SE, 2013)

$$Y_{k,j} = \bar{E}_{k,j} \cdot \frac{10\ \mathrm{MW_p}}{P_{max}} \cdot r_j \qquad \text{with } k = eq \text{ or } uq, \tag{4}$$

where the index j indicates whether a 15-min or a 1-h period was chosen. The resulting economic yield $Y_{uq,j}$ of the PV power plant was subtracted from the resulting economic yield $Y_{eq,j}$ of the PV-PCM power plant. Finally, the economic yield difference values ΔY_j were calculated by

$$\Delta Y_j = Y_{eq,j} - Y_{uq,j}, \tag{5}$$

to isolate the contribution of PCM and PCM+ in terms of economic profit or loss.

By considering the boundary conditions mentioned above, the example diurnal variations of energy economic comparisons of the PCM plant and the PCM+ plant are shown in Fig. 7. Due to the low energy yields in the morning and evening on August 2nd, the periods from 6 a.m. to 7 a.m. and from 8 p.m. to 9 p.m. were traded in 1-h blocks; the remainder was traded in 15-min blocks.

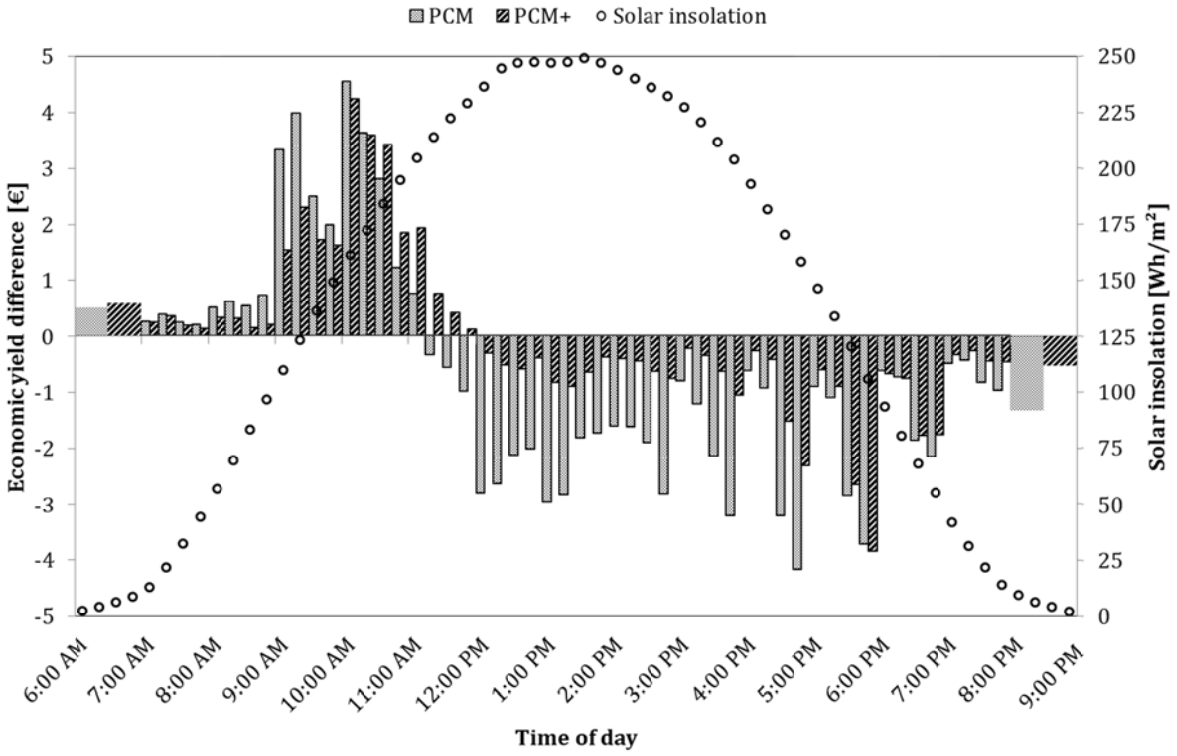

Fig. 7 Exemplary daytime dependent economic yield differences for a 10 MWp power plant of PV modules equipped with PCM or PCM+ vs. the reference PV module (baseline) on August 2nd, 2013. The solar insolation values accumulated over 15 min are superimposed on the graph.

3.4. Daily energy economic comparison

These yield differences were used to determine two comparison values for each plant configuration and day. Therefore, the energy yields $\bar{E}_{eq}$ and $\bar{E}_{uq}$ as well as the economic yields $Y_{eq,j}$ and $Y_{uq,j}$ were summed for the daytime period from 6 a.m. to 9 p.m.

$$\bar{E}_{k,d} = \sum_{i=6\ a.m.}^{9\ p.m.} \bar{E}_{k,i} \qquad \text{with } k = eq \text{ or } uq, \tag{6}$$

$$Y_{k,d} = \sum_{i=6\ a.m.}^{9\ p.m.} Y_{k,i} \qquad \text{with } k = eq \text{ or } uq. \tag{7}$$

Thus, the daily energy yield of the PV power plant was subtracted from the daily energy yield of the PV-PCM power plant. To obtain the relative comparison value e_d, the particular difference was divided by the daily energy yield of the PV power plant

$$e_d = \frac{\bar{E}_{eq,d} - \bar{E}_{uq,d}}{\bar{E}_{uq,d}} \tag{8}$$

The second relative comparison value y_d was determined analogously, i.e., using the daily economic yield values instead

$$y_d = \frac{Y_{eq,d} - Y_{uq,d}}{Y_{uq,d}}. \quad (9)$$

In addition to these daily values, the four comparison values were calculated individually for the charging and saturation stages on August 2nd, 2013, as shown in Fig. 8. It should be noted that the relative differences shown in Fig. 8 are normalized by the total yields of the corresponding stages, as shown in Fig. 5.

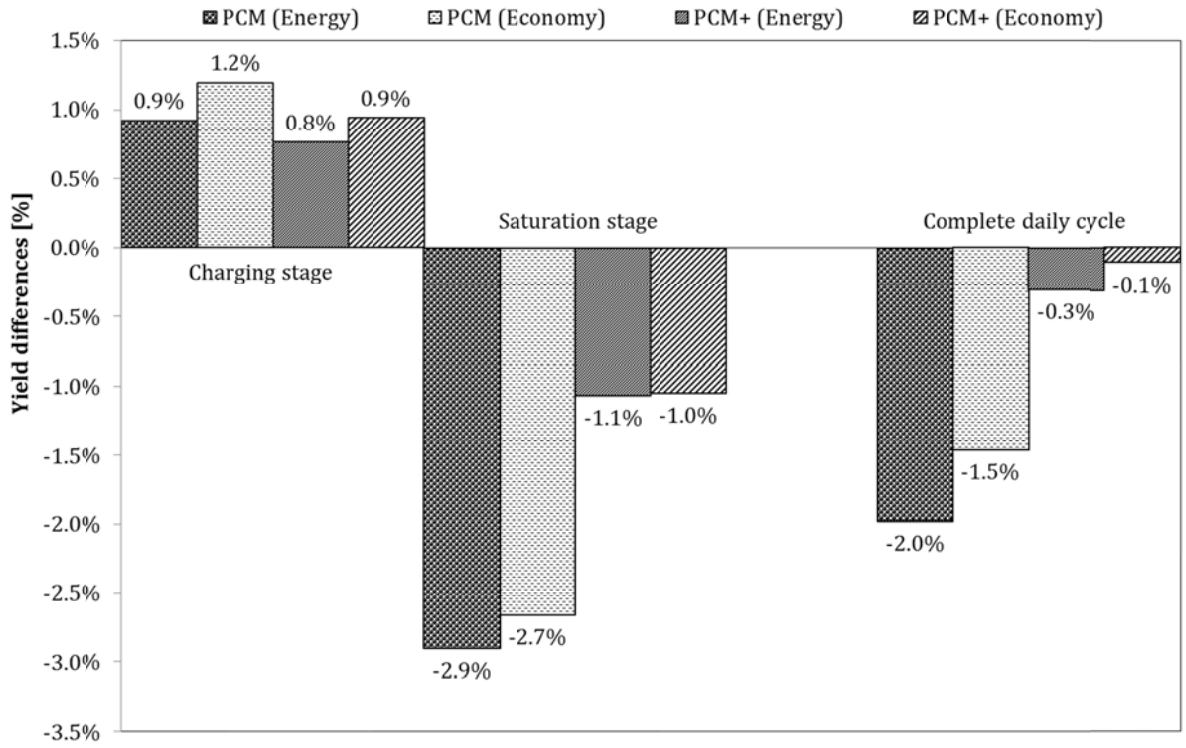

Fig. 8 Exemplary relative energy and economic yield differences for a 10 MWp power plant of PV modules equipped with PCM or PCM+ vs. the reference PV module (baseline) on August 2nd, 2013.

To compare the use of the different PCMs in terms of profitability, the economic yield was accumulated over the day trading period, cf. Fig. 9. Although the PCM+ plant achieved a smaller profit than the PCM plant before noon, over the entire trading period, the PCM+ plant was generating more profit than the PCM plant for almost 4 h.

The PCM-related increase due to high energy prices before noon on the one hand and the temperature-related power yield reduction in the afternoon due the thermal insulation effect on the other hand is clearly visible.

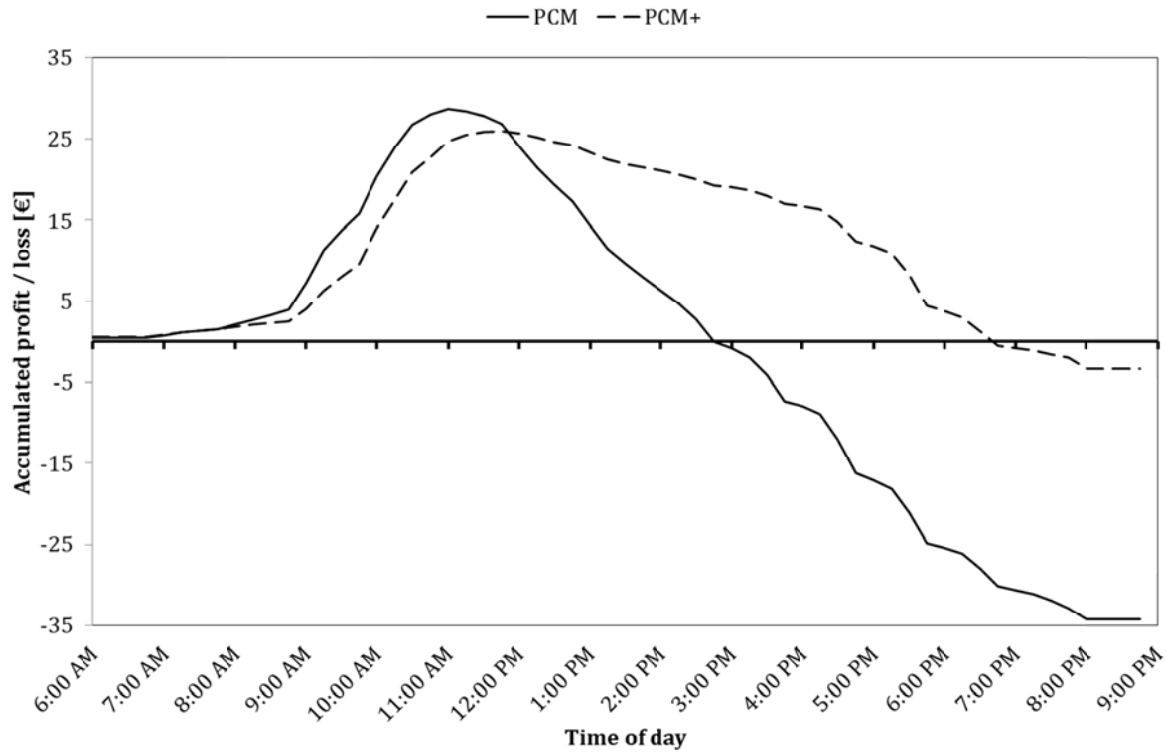

Fig. 9 Accumulated economic profit or loss of a 10 MWp PCM and PCM+ plant according to EPEX spot market prices on August 2nd, 2013.

4. Results and discussion

All of the days within the measurement period were evaluated in the same way as described above. A summarized overview of the results for each day and the daily solar insolation at the PV module level is given in Fig. 10.

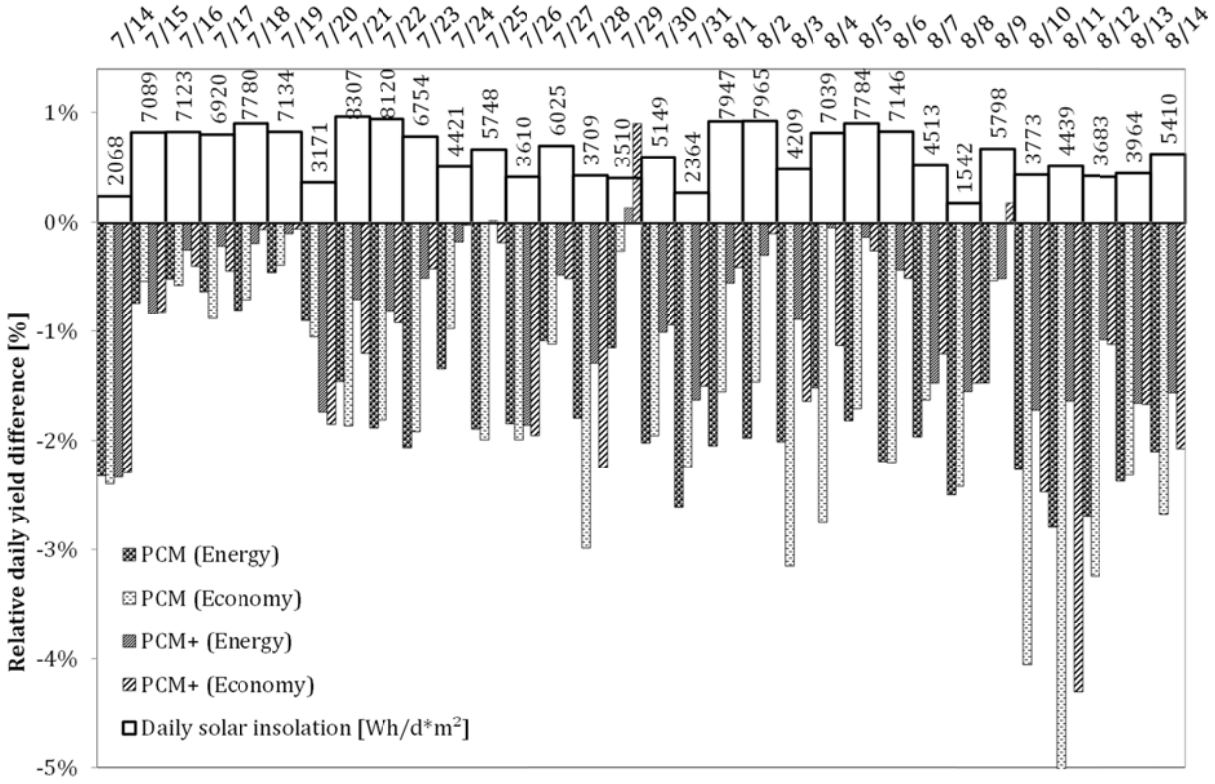

Fig. 10 Relative daily energy and economic yield differences comparing the reference PV modules with PCM and PCM+ modules during the period of July 14th, 2013 to August 14th, 2013. The cumulative daily solar insolation is illustrated with an additional bar graph.

The main findings of this comparison are as follows:

- Regarding the cumulative daily solar insolation and the yield differences, no significant interdependency has been observed.
- A decrease in energy yield was observed for both PCM and PCM+ during almost the entire measurement period. For two days only, PCM+ indicated a slight increase in energy yield.
- PCM+ yielded more energy than PCM on 28 of the 32 days because of its higher thermal conductivity producing a lower temperature.
- A decrease in economic yield was observed for both PCM and PCM+ during almost the entire measurement period. For two days only, PCM+ indicated a slight increase in economic yield.
- Higher energy prices before noon lead to a better economic yield of PCM during that period on 16 of the 32 days. The same holds for PCM+ for 14 of the 32 days.

As an additional layer on the back of the PV module, both PCM and PCM+ act as a partial thermal insulation to the environment. Therefore, their operating temperatures increased above the temperature of the reference PV module after the PCM melted. In this

light, an increase in thermal mass could be considered. However, further improvements of the thermal conductivity or optimization of the heat transfer on the back side of the PV-PCM module seems to be more appropriate. A short study, exemplified for both days discussed above, is showing that: The minimum mass increase of PCM, respectively PCM+, to reach the economic threshold has been assessed: To do so, the measured operating temperature curves of the charging stages of PCM and PCM+ have been linearly interpolated. As a result, a minimum mass increase of about 50% has been found for the PCM+. In addition, it was found out that under those circumstances PCM never may reach an economic feasible threshold. Therefore, a maximum mass increase of about 70% has been identified; that limit is given by the intercept point of the reference temperature and the trend line of the operating temperature. Using
those numbers, the following improvements in relative daily economic yield occur:
01.08.2013: PCM from -1.55% to -1.07%; PCM+ from -0.41% to 0.001%.
02.08.2013: PCM from -1.46% to -0.87%; PCM+ from -0.1% to 0.278%.

5. Conclusion

The assumption that a PV module equipped with a layer of phase change material on its back side can achieve a better economic yield than a standard PV module was evaluated for a specific configuration. Despite promising results before noon, the resulting daily energy and economic yields were almost all negative. In the studied configuration, higher prices for electricity on the spot market in the morning combined with the higher energy yield during that period are not sufficient for profitability. However, the phase change material with a higher thermal conductivity is more appropriate for a PV module application than a conventional phase change material. Next, higher energy prices on the EPEX spot market in the morning provide better results than considering the sum of daily generated electricity only.

To further investigate the economic feasibility of different configurations, the energy-economic tradeoff between thermal conductivity, heat storage capacity and resulting layer thickness as well as the back side heat transfer of the PCM with respect to the related costs should be investigated and optimized via computational simulations and evaluated based on enhanced prototypes.

References

Atkin, P., Farid, M.M., 2015. Improving the efficiency of photovoltaic cells using PCM infused graphite and aluminium fins. Solar Energy 114, 217–228.

Bahaidarah, H., Subhan, A., Gandhidasan, P., Rehman, S., 2013. Performance evaluation of a PV (photovoltaic) module by back surface water cooling for hot climatic conditions. Energy 59, 445–453.

Browne, M.C., Norton, B., McCormack, S.J., 2015. Phase change materials for photovoltaic thermal management. Renewable and Sustainable Energy Reviews 47, 762–782.

EPEX Spot SE, 2013. EPEX Intraday Market Data. https://www.epexspot.com/en/market-data/. Accessed 26 June 2016.

Hasan, A., McCormack, S., Huang, M., Norton, B., 2014. Energy and Cost Saving of a Photovoltaic-Phase Change Materials (PV-PCM) System through Temperature Regulation and Performance Enhancement of Photovoltaics. Energies 7 (3), 1318–1331.

Hasan, A., McCormack, S.J., Huang, M.J., Sarwar, J., Norton, B., 2015. Increased photovoltaic performance through temperature regulation by phase change materials: Materials comparison in different climates. Solar Energy 115, 264–276.

Huang, M., Eames, P., Norton, B., Hewitt, N., 2011. Natural convection in an internally finned phase change material heat sink for the thermal management of photovoltaics. Solar Energy Materials and Solar Cells 95 (7), 1598–1603.

Jay, A., Clerc, S., Boillot, B., Bontemps, A., Jay, F., 2010. Use of phase change material in order to maintain the temperature of integrated PV modules at a reasonable level, in: Proceedings of the 25th European Photovoltaic Solar Energy Conference and Exhibition. WIP Renewable Energies, pp. 4125–4128.

Junsangsri, P., Lombardi, F., 2010. Time/Temperature Degradation of Solar Cells under the Single Diode Model, in: Proceedings of the IEEE 25th International Symposium on Defect and Fault Tolerance in VLSI Systems (DFT). IEEE, pp. 240–248.

Kenfack, F., Bauer, M., 2014. Innovative Phase Change Material (PCM) for Heat Storage for Industrial Applications. Energy Procedia 46, 310–316.

Köntges, M., Kurtz, S., Packard, C., Jahn, U., Berger, K.A., Kato, K., Friesen, T., Iseghem, M. Van, 2014. Review of Failures of Photovoltaic Modules Report IEA-PVPS T13-01:2014. http://www.isfh.de/institut_solarforschung/task13.php. Accessed 26 June 2016.

Krauter, S., 2004. Increased electrical yield via water flow over the front of photovoltaic panels. Solar Energy Materials and Solar Cells 82 (1-2), 131–137.

Mehling, H., Cabeza, L.F., 2008. Heat and cold storage with PCM. An up to date introduction into basics and applications. Springer, 316 pp.

Mehling, H., Hiebler, S., Ziegler, F., 2000. Latent heat storage using a PCM-graphite composite material, in: Benner, M. (Ed.), Proceedings of TERRASTOCK 2000. 8th International Conference on Thermal Energy Storage, Stuttgart, pp. 375–380.

Meyer, E.L., van Dyk, E.E., 2004. Assessing the Reliability and Degradation of Photovoltaic Module Performance Parameters. IEEE Trans. Rel. 53 (1), 83–92.

Moharram, K.A., Abd-Elhady, M.S., Kandil, H.A., El-Sherif, H., 2013. Enhancing the performance of photovoltaic panels by water cooling. Ain Shams Engineering Journal 4 (4), 869–877.

Norton, B., Eames, P.C., Mallick, T.K., Huang, M.J., McCormack, S.J., Mondol, J.D., Yohanis, Y.G., 2011. Enhancing the performance of building integrated photovoltaics. Solar Energy 85 (8), 1629–1664.

Radziemska, E., 2006. Effect of temperature on dark current characteristics of silicon solar cells and diodes. Int. J. Energy Res. 30 (2), 127–134.

Sarwar, J., Mansoor, B., 2016. Characterization of thermophysical properties of phase change materials for non-membrane based indirect solar desalination application. Energy Conversion and Management 120, 247–256.

Sonnenrein, G., Elsner, A., Baumhögger, E., Morbach, A., Fieback, K., Vrabec, J., 2015. Reducing the power consumption of household refrigerators through the integration of latent heat storage elements in wire-and-tube condensers. International Journal of Refrigeration 51, 154–160.

Stultz, J.W., Wen, L.C., 1977. Thermal performance testing and analysis of photovoltaic modules in natural sunlight. LSA Task Report 5101-31. Jet Propulsion Laboratory, Pasadena, California.